Direct Torque Model Predictive Control of a Poly-Phase Permanent Magnet Synchronous Motor with Current Harmonic Suppression and Loss Reduction

Benjamin Cao[1], Brandon M. Grainger[1], Xin Wang[2], Yu Zou[3], Zhi-Hong Mao[1]
University of Pittsburgh - Electric Power Systems Laboratory - Pittsburgh, Pennsylvania USA[1]
Southern Illinois University - Department of Electrical & Computer Engineering - Edwardsville, Illinois USA[2]
Saginaw Valley State University - Department of Electrical & Computer Engineering - Saginaw, Michigan USA[3]
boc19@pitt.edu / bmg10@pitt.edu

***Abstract*— Poly-phase permanent magnet synchronous motors (PMSM) are often found valuable in more electric aerospace and military vehicle applications because of the merits of being fault tolerant, exhibiting high energy density as well as operating at high speeds. This paper presents the Direct Torque Model Predictive Control (DT-MPC) of a five-phase PMSM. Through a proposed cost function, this control method improves the large torque ripple issue in the traditional direct torque control motor drives, and more importantly, it exhibits the advantage of significantly reducing poly-phase PMSM's high order harmonics and overall system losses.**

***Keywords*—** *Loss reduction, Model predictive control, Polyphase machines, Permanent magnet synchronous motor*

I. Introduction

The more electric aerospace and military applications require the electric motor utilized to be superior in terms of fault tolerance, torque delivery/speed control quality, system heat loss minimization and exhibits high energy density. A poly-phase PMSM is an appropriate solution to address most of these needs [1]. Among different electric motor control methods, the classical direct torque control (DTC) [2] delivers very fast torque transient performance. DTC also boasts the advantages of using an easily implementable hysteresis look-up table and requires less signal transformations. However, this method is prone to introducing large current and torque ripples, which may cause system resonance. Many researchers have proposed methods for improving the classical DTC method. Methods of using a combination of space vector PWM and DTC [3], artificial intelligence [4] or using an optimized switching table [5] are found in recent literature. However, the majority of the approaches have either increased the implementation complexity, required additional parameter tuning, introduced an offline switching table generation burden or lacked control robustness. Among the latest control technologies, the DT-MPC has become an emerging choice for motor drive applications [6]-[7] and has generated fruitful industrial solutions [8].

Most of the recent published results related to MPC were focused on three-phase industrial motor drives [6]-[8]. Poly-phase (more than three phases) permanent magnetic AC motors are commonly used in safety critical applications and the MPC's performance has not been extensively studied on these motor types. This work will address this need. It turns out that, by incorporating the torque, flux, as well as the third order harmonic current into the MPC's cost function, the method proposed in this paper can significantly reduce the motor's current harmonics, system losses and improve torque response quality.

The remainder of this manuscript is summarized as follows: the model development for a five-phase PMSM and drive system is presented in Section II, the proposed DT-MPC method is described in Section III, and hardware-in-the-loop simulations for validating the proposed method is presented in Section IV, followed by a conclusion in Section V.

II. Modeling of Five Phase Permanent Magnet Synchronous Motor Drive System

The voltage equations in the five-phase stator stationary reference frame are:

$$v_{uvwxys} = r_s i_{uvwxys} + p\Lambda_{uxwxys} \tag{1}$$

$$\Lambda_{uxwxys} = \Lambda_{uxwxys\_s} + \Lambda_{uxwxys\_m} = L_s i_{uvwxys} + \Lambda_{uxwxys\_m} \tag{2}$$

where r_s, v_{uvwxys}, i_{uvwxys} and Λ_{uxwxys} are the five phase PMSM stator resistance, voltage, current and flux linkage, respectively, and p is the differential operator. Λ_{uxwxys} includes the flux linkage generated by stator current Λ_{uxwxys_s} and permanent magnetic Λ_{uxwxys_m}.

$$T_{5to2} = \frac{2}{5}\begin{bmatrix} \cos\theta & \cos(\theta-\frac{2\pi}{5}) & \cos(\theta-\frac{4\pi}{5}) & \cos(\theta+\frac{4\pi}{5}) & \cos(\theta+\frac{2\pi}{5}) \\ \sin\theta & \sin(\theta-\frac{2\pi}{5}) & \sin(\theta-\frac{4\pi}{5}) & \sin(\theta+\frac{4\pi}{5}) & \sin(\theta+\frac{2\pi}{5}) \\ \cos\theta & \cos(\theta+\frac{4\pi}{5}) & \cos(\theta-\frac{2\pi}{5}) & \cos(\theta+\frac{2\pi}{5}) & \cos(\theta-\frac{4\pi}{5}) \\ \sin\theta & \sin(\theta+\frac{4\pi}{5}) & \sin(\theta-\frac{2\pi}{5}) & \sin(\theta+\frac{2\pi}{5}) & \sin(\theta-\frac{4\pi}{5}) \\ \frac{1}{\sqrt{2}} & \frac{1}{\sqrt{2}} & \frac{1}{\sqrt{2}} & \frac{1}{\sqrt{2}} & \frac{1}{\sqrt{2}} \end{bmatrix} \tag{3}$$

$$T_{5to2} v_{uxwxys} = r_s T_{5to2} i_{uxwxys} + T_{5to2} p(L_s T_{5to2}^{-1} T_{5to2} i_{uxwxys}) + T_{5to2} p T_{5to2}^{-1} T_{5to2} \Lambda_{uxwxy\_m} \tag{4}$$

$$\begin{aligned} v_{dqs} &= T_{5to2}v_{uvwxys} \\ i_{dqs} &= T_{5to2}i_{uvwxys} \\ \Lambda_{dqs} &= T_{5to2}\Lambda_{uvwxys} \end{aligned} \quad (5)$$

$$v_{dqs} = r_s i_{dqs} + L_{dqs} p i_{dqs} + \omega\Gamma_{dqs} i_{dqs} + e_{dqs} \quad (6)$$

$$L_{dqs} = T_{5to2}L_s T_{5to2}^{-1};\ \Gamma_{dqs} = T_{5to2}\frac{\partial L_s}{\partial\theta}T_{5to2}^{-1} + T_{5to2}L_s\frac{\partial T_{5to2}^{-1}}{\partial\theta};\ e_{dqs} = T_{5to2}\frac{\partial T_{5to2}^{-1}}{\partial\theta}\omega\Lambda_{dqs\_m} + T_{5to2}p\Lambda_{dqs\_m}$$

Equation (3) is the Park transformation for a 5-phase system. Applying (3) to (1) and (2), the five phase stationary sinusoid variables can be equivalently represented as a rotating DC space vector through Park's transformation as shown from (4)-(6). Note a few preliminary steps are listed as (4) and (5) for mapping the five phase system into the two phase system for the interested reader. Based on [9], the five-phase PMSM could be equivalently expressed as two sets of reference frames defined as *d1-q1* and *d3-q3* seen in Fig. 1. Note that the *d1-q1* reference frame represents the (10n±1)th harmonics rotating counterclockwise at speed ω, while the *d3-q3* reference frame represents (10n±3)th harmonics rotating counterclockwise at a speed of 3ω.

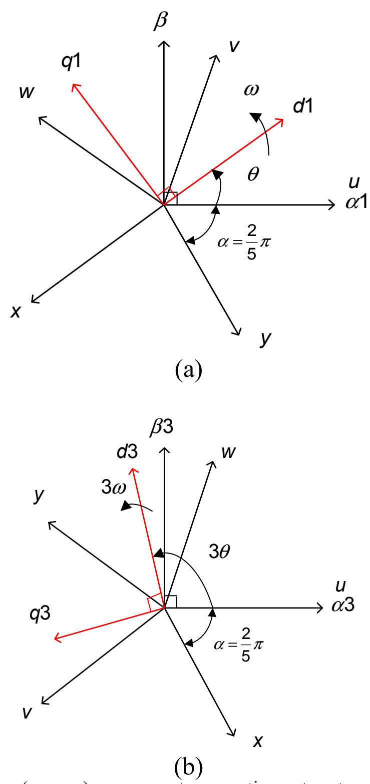

Fig. 1.Five phase (uvwxy) permanent magnetic motor, two phase stationary ($\alpha\beta$) and two rotational reference frame. The figure at the top shows the *d1-q1* frame of reference and the figure in the bottom shows the *d3-q3* frame of reference [9].

A. *Motor Drive System Modeling Incorporating Motor Copper Loss, Iron Loss, and Power Inverter Switching Loss*

The equivalent circuit model considering motor copper and core loss is depicted as Fig. 2. The core loss is represented as a resistance across the rotor branch, r_c, of the well-known "T" circuit model of a PM AC motor.

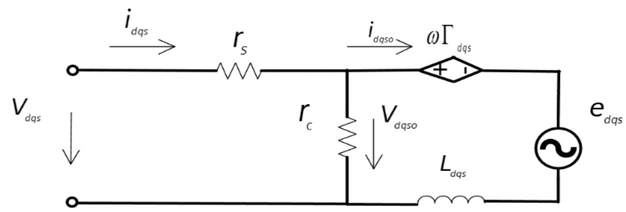

Fig. 2.Five phase PM motor equivalent circuit.

The outer loop voltage and current are defined by:

$$V_{dqs} = r_s i_{dqs} + V_{dqso} \quad (7)$$

$$i_{dqs} = i_{dqso} + \frac{V_{dqso}}{r_c} \quad (8)$$

The internal loop voltage is defined by:

$$V_{dqso} = \omega\Gamma_{dqs} + e_{dqs} + L_{dqs} p i_{dqso} \quad (9)$$

Substituting (8) into (7), one arrives at

$$V_{dqs} = r_s\left(i_{dqso} + \frac{V_{dqso}}{r_c}\right) + V_{dqso} = r_s i_{dqso} + \left(1 + \frac{r_s}{r_c}\right)V_{dqso} \quad (10)$$

Substituting (9) and (10) into (7), the new motor relationship incorporating copper and iron loss is listed as (11), where v_{dqs} is the stator voltage in the *dq* frame of reference; r_s and r_i are the resistance for stator and iron loss respectively; i_{dqso} is the stator current contributing to energy conversion after subtracted iron loss current, and e_{dqs} is the back emf in the *dq* frame of reference.

$$\left(\frac{r_i}{r_s + r_i}\right)v_{dqs} = \left(\frac{r_i}{r_s + r_i}\right)r_s i_{dqso} + \omega\Gamma_{dqs} + e_{dqs} + L_{dqs} p i_{dqso} \quad (11)$$

The total power loss in power inverters is the summation of the semiconductor device switching and conduction losses. Power semiconductor switching losses can be modelled by (12), [7]. In (12), N is the number of transistors in the inverter, T_c is the duration of the commutation for one transistor in one control cycle, $i_c(t)$, $v_{ce}(t)$ are the current on the collector and voltage across collector/emitter on the transistor, respectively.

$$L_{sw} = \sum_{j=1}^{N}\int_{T_c} i_c(t)v_{ce}(t)dt \quad (12)$$

III. The Proposed DT-MPC And Cost Function

A. *Cost Function and Control Flow*

The overall DT-MPC based motor drive system is shown in Fig. 3. The direct torque model predictive controller (DT-MPC) input signals include motor torque and flux reference current commands I_{qs1}^* and I_{ds1}^*, respectively, as well as the third order harmonic current reference commands I_{qs3}^* and I_{ds3}^*.

The output signals from the DT-MPC controller are the gate signals for the IGBT inverter, which controls the torque and speed of the five-phase permanent magnet AC motor.

We propose a new cost function, based on the principle of minimizing the overall system losses including power inverter switching loss, motor copper loss, and iron losses. More importantly, the third order harmonic current I_{qs3} and I_{ds3} can be suppressed, while keeping the flux producing current I_{ds1} and torque producing current I_{qs1} inside a predefined hysteresis band. The proposed DT-MPC cost function is given by (13). Note that x represents the available voltage space vector commands, L_{sw} and L_{motor} denote the inverter switching loss and electric motor loss, respectively. Note that λ is a weighing factor used for third harmonic current suppression. When we set $\lambda = 0$ in the cost function, the third order harmonic suppression capability is turned off. On the other hand, when we set $\lambda = 1$, the DT-MPC controller is designed to minimize the third order harmonic content in the output current waveforms. ε_{limit} is the hysteresis band tolerance level for limiting the torque and flux current error.

As shown in the flow chart diagram of Fig. 4, to implement the proposed DT-MPC algorithm, at an arbitrary k_{th} time instant, the reference commands are computed and output signals are measured. We obtain the state space variable values at the k_{th} time step based on discretizing the system dynamic equation, (11), and considering delay compensation [7]. Meanwhile, the cost function is evaluated and stored for determining the optimal voltage space vector command for the IGBT based inverter. The procedure is then repeated for the next k+1th sampling time step.

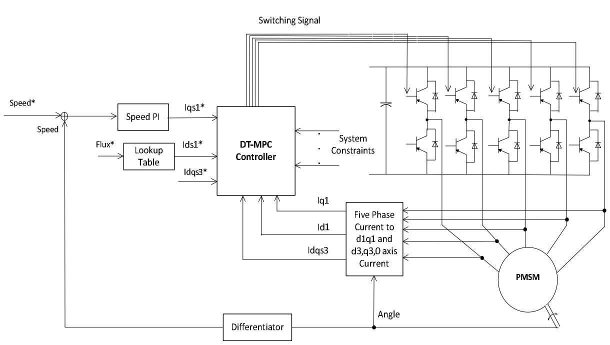

Fig. 3. Control loop diagram for a Five-Phase PMSM motor drive.

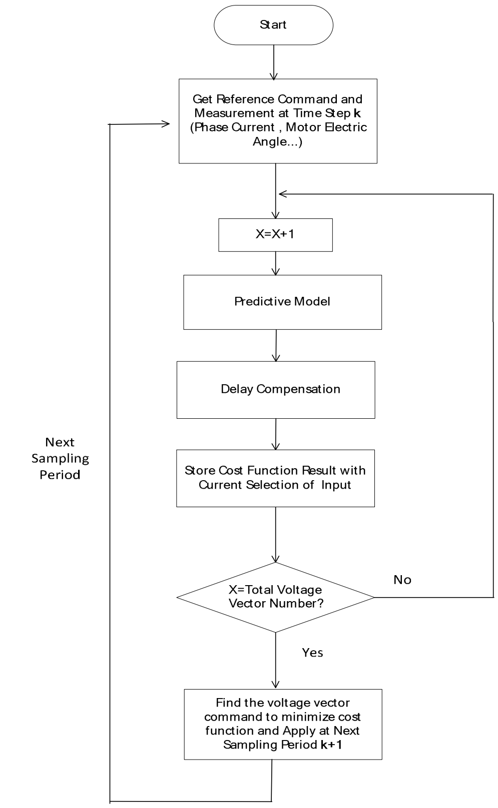

Fig. 4. DT-MPC algorithm with logic flow.

B. *Delay Compensation through Linear Interpolation*

Delay compensation is implemented through linear interpolation between predictions at step k+1 and step k+2. It is applied to select the feasible control command, which is chosen to minimize the cost function and compensate calculation delay, while restricting the control variables within the hysteresis band. Fig.5 through 8 demonstrate four different scenarios of generating the control command. In Case I, the generated control commands will be abandoned, since the predictions are out of the bound, and the trend is deviating away from the hysteresis band. In Case III, the control command, which could minimize system cost function, will be selected. In Case II and IV, a linear interpolation of the two data points is used to estimate the control command. This procedure is important for minimizing the system cost function as it can avoid unnecessary converter switching loss and motor loss. The coefficients a and b of the linear equation are determined based on the two estimations. The control command will be determined by the intersection (marked in red) between the linear equation and the bound of hysteresis band.

$$V_p^{OPT}(x_{k+1}) = \min\{L_{sw}(x_k \ldots x_{k+N-1}) + L_{motor}(x_k \ldots x_{k+N-1})\} + \lambda * \min\{\left|(i^*_{ds3\_k+1} - i_{ds3\_\_k+1\ldots k+N-1})\right| + \left|(i^*_{qs3\_k+1} - i_{qs3\_\_k+1\ldots k+N-1})\right|\} \quad (13)$$

Subject to:

$$\begin{bmatrix} \left| i^*_{ds1\_k+1} - i_{ds1\_\_k+1\ldots k+N-1} \right| \\ \left| i^*_{qs1\_k+1} - i_{qs1\_\_k+1\ldots k+N-1} \right| \end{bmatrix} \le \varepsilon_{\lim it}$$

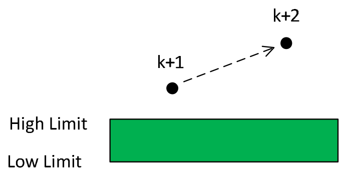

Fig. 5. Case I (Abandoned): Both predictions are out of the boundary and the trend is moving away from hysteresis band.

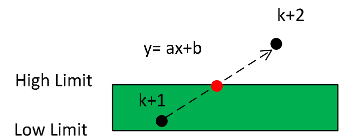

Fig. 6. Case II (Linear Interpolation): One prediction is within the boundary.

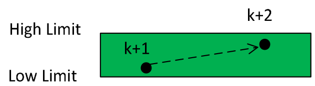

Fig. 7. Case III: Both predictions are within the boundary.

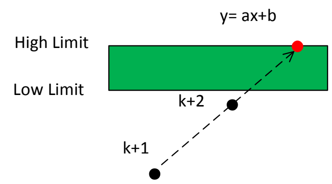

Fig. 8. Case IV (Linear Interpolation): Both predictions are out of the boundary but the trend is moving towards the hysteresis band.

IV. Hardware-In-The-Loop Results

Three control methods are compared including classic DTC, DT-MPC without harmonic suppression by setting $\lambda = 0$, and DT-MPC with third harmonic current suppression by setting $\lambda \neq 0$. Opal-RT OP5600 hardware in the loop system was utilized to evaluate and compare the performance of the three approaches. The torque and speed are sampled at frequencies of 40 kHz and 2 kHz, respectively. The parameters of the five-phase PMSM and electric drive are listed in Table I.

TABLE I.
DRIVE PARAMETERS

System Parameter	Value
Stator Resistance	0.416 Ω
Iron Loss Resistance	100 Ω
Stator Inductance	1.365 mH
No. of pole pairs	2
Flux linkage constant	0.117 Wb-t
Electric Drive DC Voltage	500 V
Electric Drive Maximum Phase Current	100 A
Electric Drive Single Switching Loss	1 mJ

TABLE II.
LOSS PARAMETERS OF THREE TECHNIQUES

Loss Comparison	Motor Copper Loss	Motor Iron Loss	Switching Loss
Classic DTC	1	1	1
DT-MPC Without Third Harmonics Current Suppression	0.72	0.5	0.5
DT-MPC Without Third Harmonics Current Suppression	0.28	0.5	0.4

First, the average loss comparison among the three methods in per unit (classic DTC loss is defined to be the base value) is summarized in Table II. The total system loss with the proposed DT-MPC with harmonic suppression shows a significant system loss reduction compared with classic DTC, including about 70% reduction in copper loss, 50% reduction in iron loss and 40% in switching loss. Particularly, in Fig. 9, the significant copper loss reduction from the proposed DT-MPC is confirmed, specifically caused by a reduction in the phase current magnitude as shown in Fig. 10. In addition, the speed and torque regulations are presented in Fig. 11 and Fig. 12, respectively. In Fig. 11, the accuracy of the motor speed under the proposed DT-MPC is comparable to the traditional DT-MPC, both of which are superior in performance compared to the classic DTC results. To further validate the dynamic performance, a step torque command is employed and the torque responses are compared among the three methods as shown in Fig. 12. While the motor torque follows the reference accurately, more torque ripple is noticed in the proposed DT-MPC method with harmonic suppression compared to the DT-MPC without harmonic suppression.

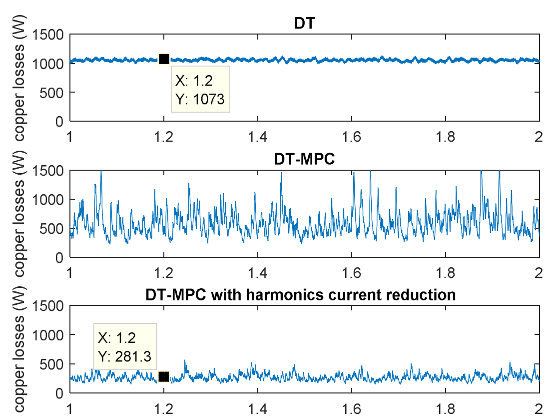

Fig. 9. Copper loss comparison with the DT, DT-MPC, and the proposed DT-MPC with harmonic current reduction method.

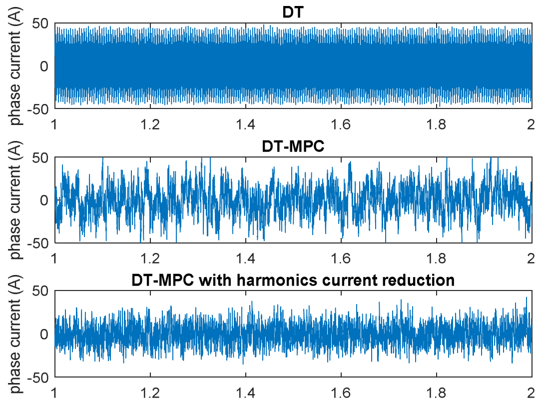

Fig. 10. Phase current comparison with the DT, DT-MPC, and the proposed DT-MPC with harmonic current reduction method.

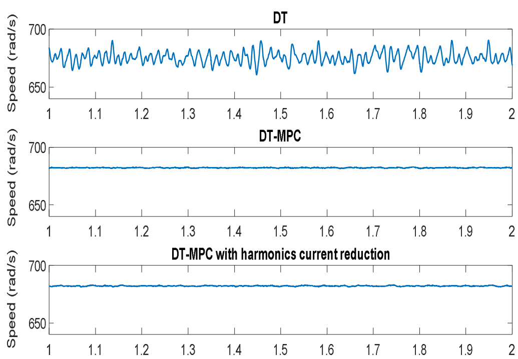

Fig. 11. Motor speed response comparison with the DT, DT-MPC, and the proposed DT-MPC with harmonic current reduction method.

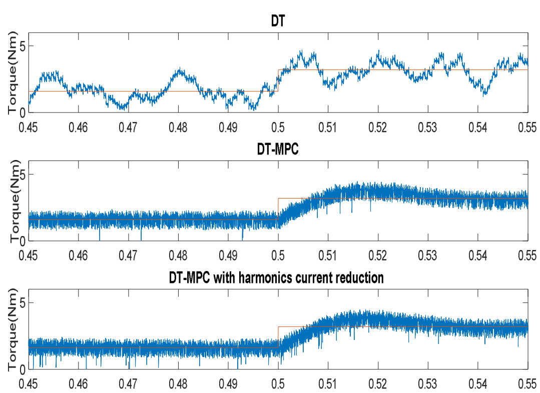

Fig. 12. Motor torque response comparison with the DT, DT-MPC, and proposed DT-MPC with harmonic current reduction method.

V. Conclusion

This paper presents a new DT-MPC with harmonic current suppression and loss minimization cost function. By including the 3rd order harmonic suppression, the proposed DT-MPC approach effectively addresses the high torque ripple issue in the traditional DTC and more importantly, shows a significant advantage of loss reduction compared to the traditional DT-MPC without harmonic suppression. Opal-RT OP5600 HIL system was used to verify the efficacy of the approach and the results exhibit significant improvement in reducing PMSM losses.

References

[1] K. Rajashekara, "Parallel between More Electric Aircraft and Electric/Hybrid Vehicle Power Conversion Technologies," *IEEE Electrification Magazine*, vol. 2, no. 2, pp. 50-60, June 2014.

[2] I. Takahashi and T. Noguchi, "A New Quick response and high Efficiency Strategy of an Induction Motor," *IEEE Transactions on Industry Applications*, vol. 22, no. 5, 1986, pp. 820–827, Sept. 1986.

[3] C.Lascu, I.Boldea, F.Blaabjerg "A Modified Direct Torque Control for Induction Motor Sensorless Drive" I*EEE Transactions on Industry Applications*, vol. 36, no. 1, pp. 122-130, January/February, 2000.

[4] L. Romeral, A. Arias, E. Aldabas and M.G. Jayne "Novel Direct Torque Control (DTC) Scheme with Fuzzy Adaptive Torque-Ripple Reduction," *IEEE Transactions on Industrial Electronics*, vol.50, no.3, pp. 487-492, June 2003.

[5] L.Parsa and H.Toliyat, "Sensorless Direct Torque Control of Five-Phase Interior Permanent-Magnet Motor Drives", *IEEE Transactions on Industry Applications*, vol.43, no.4, pp. 952-959, July/August 2007.

[6] T.Geyer,G.Papafotiou, and M.Morari, "Model Predictive Direct Torque Control—Part I: Concept, Algorithm, and Analysis", *IEEE Transactions on Industrial Electronics*, vol.56, no.6, pp. 1894-1905, June 2009.

[7] P Cortes and J Rodriguez, "Predictive Control of Power Converters and Electrical Drives", Willey-IEEE Press, 2012.

[8] G.A.Papafotiou, G.D.Demetriades, V.G.Agelidis, "Technology Readiness Assessment of Model Predictive Control in Medium and High Voltage Power Electronics", *IEEE Transactions on Industrial Electronics*, vol.63, no.9, pp. 5807-5815, September 2016.

[9] H.Ryu,J.Kim and S.Sul, "Synchronous Frame Current Control of Multi-Phase Synchronous Motor Part I. Modeling and Current Control Based on Multiple d-q Spaces Concept Under Balanced Condition", 39th IAS Annual Meeting, 2004.